

Discrete Laplace Operator on Meshed Surfaces

Mikhail Belkin*

Jian Sun †

Yusu Wang‡

Abstract

In recent years a considerable amount of work in graphics and geometric optimization used tools based on the Laplace-Beltrami operator on a surface. The applications of the Laplacian include mesh editing, surface smoothing, and shape interpolations among others. However, it has been shown [12, 23, 25] that the popular cotangent approximation schemes do not provide convergent point-wise (or even \mathcal{L}_2) estimates, while many applications rely on point-wise estimation. Existence of such schemes has been an open question [12].

In this paper we propose the first algorithm for approximating the Laplace operator of a surface from a mesh with point-wise convergence guarantees applicable to arbitrary meshed surfaces. We show that for a sufficiently fine mesh over an arbitrary surface, our mesh Laplacian is close to the Laplace-Beltrami operator on the surface at every point of the surface.

Moreover, the proposed algorithm is simple and easily implementable. Experimental evidence shows that our algorithm exhibits convergence empirically and outperforms cotangent-based methods in providing accurate approximation of the Laplace operator for various meshes.

*Dept. of Computer Science and Engineering, The Ohio State University, Columbus, OH 43210.

†Dept. of Computer Science, Stanford University, Palo Alto, CA 94305.

‡Dept. of Computer Science and Engineering, The Ohio State University, Columbus, OH 43210.

1 Introduction

A broad range of topics in geometric modeling and computer graphics is concerned with processing two-dimensional surfaces in a three-dimensional space. These surfaces are typically represented by a mesh, which is given by the coordinates of its vertices and the connectivity information. Thus, manipulating, deforming and analyzing meshed surfaces is a crucial area within these subjects, with the usual implicit assumption that processing of a mesh corresponds to analogous processing of the underlying surface.

In recent years a class of methods based on discrete differential geometry of surfaces [1] and the discrete Laplace operator has been used for various tasks of geometric processing. For example, the state-of-the-art report on Laplacian Mesh Processing [20] discusses surface reconstruction, mesh editing, shape representation and shape interpolation among other applications of Laplacian-based mesh processing methods. Such applications of the Laplacian can be found in [2, 9, 11, 21, 22, 26] among others.

The Laplace-Beltrami operator (manifold Laplacian) is a fundamental geometric object associated to a Riemannian manifold and has many desirable properties. The Laplacian can be used as a smoothness penalty to choose functions varying smoothly along the manifold [22] or to smooth the surface itself via the *mean curvature flow* [9], which is determined by applying the Laplace operator to coordinate functions x, y, z considered as functions on the surface. Moreover, eigenfunctions of the Laplacian form a natural basis for square integrable functions on the manifold analogous to Fourier harmonics for functions on a circle (i.e. periodic functions). Therefore, computing eigenfunctions of a Laplacian allows one to construct a basis reflecting the geometry of the surface [11]. Finally, the Laplace operator is intimately related to diffusion and the heat equation on the surface, and is connected to a large body of classical mathematics, relating geometry of a manifold to the properties of the heat flow (see, e.g., [19]).

Several discretizations of the Laplacian for an arbitrary mesh have been proposed [8, 9, 13, 18, 22, 24]. Most of the proposed methods are variants of the *cotangent scheme* [18], which is a form of the finite element method, applied to the Laplace operator on a surface. Suppose we have a surface with a fine mesh. We expect that the discretization computed from such a mesh would be an accurate representation of the underlying surface Laplacian. However, a detailed theoretical analysis of existing discretizations in [24, 25] shows that while point-wise convergence can be established for special classes of meshes, such as certain meshes with valence 6, or for linear functions over a sphere in \mathbb{R}^3 , none of these methods can be expected to converge for surface meshes in general, a finding, which is borne out by experimental results in Section 5 and [25]. A notable recent work is [12, 23], where the authors analyze convergence of various geometric invariants, including Laplace-Beltrami operators. They apply their analysis to the popular cotangent scheme showing *weak convergence* (in the distribution sense) for the solution of the Dirichlet's problem, assuming the aspect ratio of mesh elements is bounded. The authors also demonstrate that under the cotangent scheme, convergence in \mathcal{L}_2 (which is weaker than point-wise convergence) does not generally hold.

The results presented in our paper provide the first discretization scheme that guarantees convergence at each point (i.e, \mathcal{L}_∞ and thus also \mathcal{L}_2 convergence). We note that while such convergence is required in many applications, where various quantities, such as mean curvature, need to be estimated at each node of the mesh, the construction of such a scheme is not trivial.¹ The contributions of the paper are as follows:

1. We propose a simple method for approximating integrals over a surface using a mesh and analyze the quality of the resulting approximation in terms of the parameters of the surface and the mesh.
2. Combining the result above with the idea of approximating the heat flow on a mesh, we present and analyze the first algorithm for approximating Laplace-Beltrami operator on a surface with point-wise convergence guarantees for arbitrary meshes (no bound on aspect ratio is required).
3. The resulting algorithm is simple and experimental results show that it significantly outperforms the cotangent scheme Laplace approximation in approximation quality and robustness to noise.

¹For example, in [12] the authors conjecture that such discretizations may not exist.

We note that the algorithm for computing the surface Laplacian is related to the set of algorithms for computing Laplacian of point clouds in data analysis and machine learning [6, 7] by using the heat equation. We observe that in machine learning, the samples are usually believed to be drawn *independently* from a probability distribution and the convergence occurs in probability. On the other hand, in surface modeling, the nodes of a mesh are typically not sampled independently from a probability distribution but are generated by some deterministic process, e.g. scanning. Hence in the case of mesh Laplacian, approximation guarantees need to be made for *all* sufficiently fine meshes, and probabilistic techniques based on the law of large numbers (usually used in the case of randomly sampled point clouds) cannot be applied.

2 Algorithm and Overview of the Results

2.1 Mesh Laplacian Algorithm

We start by describing our algorithm for computing the Laplace operator on a meshed surface. Let K be a mesh in \mathbb{R}^3 . Given a face, a mesh, or a surface X , let $\text{Area}(X)$ denote the area of X . For a face $t \in K$, the number of vertices in t is denoted by $\#t$, and $V(t)$ is the set of vertices of t .

Our algorithm takes a function $f : V \rightarrow \mathbb{R}$ as **input** and produces another function $L_K^h f : V \rightarrow \mathbb{R}$ as **output**. L_K^h , the **mesh Laplace operator**, is computed, for any $w \in V$, as follows:

$$L_K^h f(w) = \frac{1}{4\pi h^2} \sum_{t \in K} \frac{\text{Area}(t)}{\#t} \sum_{p \in V(t)} e^{-\frac{\|p-w\|^2}{4h}} (f(p) - f(w)) \quad (1)$$

The **parameter** h is a positive quantity, which intuitively corresponds to the size of the neighborhood considered at each point. In many applications and for the theoretical analysis in this paper h is taken to be independent of the point w . However, in general, h can be taken to be a function of w , which will allow the algorithm to adapt to the local mesh size.

The theoretical results in this paper show that when K is a sufficiently fine mesh of a smooth underlying surface S , L_K^h is close to the surface Laplacian Δ_S (the formal definition will be introduced shortly). Indeed, our preliminary experimental results demonstrate the converging behavior of this operator, and show that our algorithm greatly outperforms currently available discrete Laplace operators in the approximation quality.

In the remaining of this section, after introducing necessary notations, we give an outline of the theoretical results, which also explains the derivation of this algorithm.

2.2 Objects and Notations

Surface Laplace operator Δ_S . In this paper, we consider a smooth compact 2-manifold S isometrically embedded in some Euclidean space \mathbb{R}^3 with geometry induced by the embedding. The corresponding *volume form*, denoted by ν , determines the area of a surface element. We assume that S is connected — surfaces with multiple components can be handled by applying our results in a component-wise manner.

Given a twice continuously differentiable function $f \in C^2(S)$, let $\nabla_S f$ denote the gradient vector field of f on S . The Laplace-Beltrami operator Δ_S of f is defined as the divergence of the gradient; that is, $\Delta_S f = \text{div}(\nabla_S f)$. If S is a domain in \mathbb{R}^2 , the Laplacian has the familiar form $\Delta_{\mathbb{R}^2} f = \frac{\partial^2 f}{\partial x^2} + \frac{\partial^2 f}{\partial y^2}$.

Functional Laplacian F_S^h . To connect the mesh Laplace operator L_K^h , as defined in Eqn (1), with the surface Laplacian Δ_S , we need an intermediate object, called the *functional Laplace operator* F_S^h . Given a point $w \in S$ and a function $f : S \rightarrow \mathbb{R}$, it is defined as follows:

$$F_S^h f(w) = \frac{1}{4\pi h^2} \int_{x \in S} e^{-\frac{\|x-w\|^2}{4h}} (f(x) - f(w)) d\nu(x). \quad (2)$$

Definition of (ϵ, η) -approximation. We also need a quantitative measure of how well a mesh approximates the underlying surface. Let the *medial axis* M of S be the closure of the set of points in \mathbb{R}^3 that have at least two closest points in S . For any $w \in S$, the *local feature size at w* , denoted by $\text{lfs}(w)$, is the distance from w to the medial axis M . The *reach* (also known as the condition number) $\rho(S)$ of S is the infimum of the local feature size at any point in S . At each point $p \in S$, n_p denotes the *unit outward normal* of S at p and for each face $t \in K$, n_t is the unit outward normal of the plane passing through t .

A mesh K approximates the surface S if the vertices of K are in S . Let ρ be the reach of S . We say that K is an (ϵ, η) -approximation of S , if the following conditions hold:

1. For a face $t \in K$, its diameter (maximum distance between any two points on t) is at most $\epsilon\rho$.
2. For a face $t \in K$ and a vertex $p \in t$, the angle between vectors n_t and n_p , $\angle(n_t, n_p)$, is at most η .

Intuitively, the first condition ensures that the mesh is sufficiently fine. On the other hand, a very fine mesh can still provide a poor approximation to the underlying surface, as, for example, is seen in the Schwartz lantern. Thus the second condition is also necessary to ensure the closeness between K and S . Note that many surface reconstruction algorithms (see [10]) produce meshes that satisfy these conditions.

Finally, we introduce the map $\phi : K \rightarrow S$. For any $p \in K$, $\phi(p)$ is defined as the closest point to p on the surface S . ϕ is well-defined when K avoids the medial axis of S , which will be the case in our setting. The map ϕ connects the mesh K with the surface S , and is widely used in analyzing surface reconstruction algorithms [3, 10], as well as in approximating various quantities for smooth surfaces [12, 15].

2.3 Overview of Main Results

Our main result is Theorem 2.1. Intuitively, as the mesh approximating the surface S becomes denser, the mesh Laplace operator on K converges to the Laplace-Beltrami operator of S .

Theorem 2.1 *Let the mesh $K_{\epsilon, \eta}$ be an (ϵ, η) -approximation of S . Put $h(\epsilon, \eta) = \epsilon^{\frac{1}{2.5+\alpha}} + \eta^{\frac{1}{1+\alpha}}$ for an arbitrary fixed positive number $\alpha > 0$. Then for any $f \in C^3(S)$*

$$\lim_{\epsilon, \eta \rightarrow 0} \sup_{K_{\epsilon, \eta}} \left\| \mathbb{L}_{K_{\epsilon, \eta}}^{h(\epsilon, \eta)} f - \Delta_S f \right\|_{\infty} = 0 \quad (3)$$

where the supremum is taken over all (ϵ, η) approximations of S .

The proof of Theorem 2.1 relies on the following two results, connecting the mesh Laplacian operator to the functional Laplace operator and the functional Laplacian to the Laplace-Beltrami operator, respectively.

Theorem 2.2 *Let K be an (ϵ, η) -approximation of the surface S , and $\epsilon, \eta < 0.1$. Given a function $f \in C^1(S)$, let $\|f\|_{\infty} = \sup_{x \in S} |f(x)|$, $\|\nabla f\|_{\infty} = \sup_{x \in S} \|\nabla f(x)\|$ and ρ denote the reach of surface S . We have that for any point $w \in S$,*

$$\left| \mathbb{F}_S^h f(w) - \mathbb{L}_K^h(w) \right| \leq \frac{\text{Area}(S)}{\pi h^2} \left(\left(\left(1 + \frac{2\rho}{\sqrt{h}} \right) \epsilon + 6\epsilon\eta + 2\eta^2 \right) \|f\|_{\infty} + \rho\epsilon \|\nabla f\|_{\infty} \right).$$

Theorem 2.3 (See [7]) *For a function $f \in C^2(S)$, we have that $\lim_{h \rightarrow 0} \|\mathbb{F}_S^h f(w) - \Delta_S f(w)\|_{\infty} = 0$.*

It is easy to see that Theorem 2.1 follows from the two theorems above. Theorem 2.3 was shown in [7], and provides an approximation to the Laplace operator based on heat diffusion. To make it more transparent we give a brief outline of the ideas involved in Appendix A. In what follows, we focus on the proof of Theorem 2.2. The proof relies on the following result, which is of independent interest. Let $d_S(x, y)$ denote the geodesic distance between two points $x, y \in S$.

Theorem 2.4 Given a Lipschitz function $g : S \rightarrow \mathbb{R}$, let $L = \text{Lip}(g)$ be the Lipschitz constant of function g , i.e., $|g(x) - g(y)| \leq \text{Lip}(g)d_S(x, y)$. Set $\|g\|_\infty = \sup_{x \in S} |g(x)|$. We can approximate $\int_S g d\nu$ by the discrete sum $I_{Kg} = \sum_{t \in K} \frac{\text{Area}(t)}{\#t} \sum_{v \in V(t)} g(v)$, so that the following inequality holds:

$$\left| \int_S g d\nu - I_{Kg} \right| \leq 3 (\rho L \varepsilon + \|g\|_\infty (2\varepsilon + \eta)^2) \text{Area}(S). \quad (4)$$

Moreover, suppose that the mesh is triangular and g is twice differentiable, with the norm of the Hessian of g bounded by H . Then, for some constant C , depending only on S , the following inequality holds:

$$\left| \int_S g d\nu - I_{Kg} \right| \leq (CH\varepsilon^2 + 3\|g\|_\infty (2\varepsilon + \eta)^2) \text{Area}(S) \quad (5)$$

Note that in the second part of the above theorem provides a higher-order approximation, while the first part only requires the function g to be Lipschitz.

Finally, we remark that Theorem 2.2 and Theorem 2.4 still hold for a mesh K approximating S in an adaptive manner. Roughly speaking, this means that the length of any edge incident to a vertex $v \in K$ is at most ε times the local feature size at v . We describe the non-adaptive version in this paper, as it is not yet clear how to prove the adaptive version of Theorem 2.3, thus of Theorem 2.1.

3 Properties of Meshed Surfaces

In this section, we present several results on the relations between a smooth surface S and an (ε, η) -approximation K of S . For simplicity of the exposition, we assume from now on that K is a triangular mesh. However the same analysis works verbatim for arbitrary (ε, η) -approximation meshes. Let ρ be the reach of S , and $\phi : K \rightarrow S$ is the closest-point map introduced in Section 2.2.

3.1 Closeness Between S and K

Given any point $p \in \mathbb{R}^3$, let $d(p, X)$ denote the smallest distance from p to any point in the set $X \subset \mathbb{R}^3$, and n_p the unit normal of S at p . The following result from [5] bounds the surface normal variation between nearby points.

Lemma 3.1 ([5]) Given two points $p, q \in S$ with $\|p - q\| \leq \rho/3$, the angle between n_p and n_q satisfies that $\angle(n_p, n_q) < \frac{\|p - q\|}{\rho - \|p - q\|}$.

We will later need the following result bounding the geodesic distance $d_S(p, q)$ between two points $p, q \in S$, in terms of the Euclidean distance $\|p - q\|$. Note the the difference $d_S(p, q) - \|p - q\|$ is of order 3 in $\|p - q\|$, which significantly improves the quadratic bound from [16].

Lemma 3.2 Given two points $p, q \in S$, let $d = \|p - q\| < \rho/2$. Then we have that $d \leq d_S(p, q) \leq d + \frac{4d^3}{3\rho^2}$.

Proof: Let γ be the shortest geodesic curve between p and q and set $l = d_S(p, q)$. By Proposition 6.3 in [16] we have that $l \leq 2d$. For any $x \in \gamma$, let $t_x = t_x(\gamma)$ be the *unit* tangent vector of γ at x , and $\gamma[p, x]$ the portion of γ from p to x . Set $l_x = d_S(p, x)$.

Since γ is a geodesic, the unit normal of γ at a point $x \in \gamma \subseteq S$ is the same as the unit surface normal n_x at x , and the curvature of γ is upper bounded by $1/\rho$. It then follows from the Frenet Formulas that $\|dt_x/dl_x\| \leq \|n_x/\rho\|$. Hence we have that

$$\|t_x - t_p\| = \left\| \int_{\gamma[p, x]} dt_y \right\| \leq \int_{\gamma[p, x]} \left\| \frac{n_y}{\rho} \right\| dl_y \leq \frac{l_x}{\rho} \Rightarrow \sin \frac{\angle(t_p, t_x)}{2} \leq \frac{l_x}{2\rho}.$$

Furthermore, let $u \cdot v$ denote the dot-product between vectors u and v . Then we have that

$$\int_{\gamma} t_x \cdot t_p \, dl_x = \int_{\gamma} \cos \angle(t_x, t_p) \, dl_x = \int_{\gamma} \left(1 - 2 \sin^2 \frac{\angle(t_x, t_p)}{2}\right) \, dl_x \geq \int_{\gamma} \left(1 - \frac{l_x^2}{2\rho^2}\right) \, dl_x = l - \frac{l^3}{6\rho^2}$$

On the other hand, observe that $\int_{\gamma} t_x \cdot t_p \, dl_x$ measures the length of the (signed) projection of γ along the direction t_p . That is, $\int_{\gamma} t_x \cdot t_p \, dl_x = (q - p) \cdot t_p$. Hence we have that

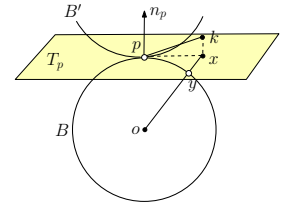
$$d = \|p - q\| \geq (q - p) \cdot t_p \geq l - \frac{l^3}{6\rho^2} \Rightarrow l \leq d + \frac{l^3}{6\rho^2} \leq d + \frac{4d^3}{3\rho^2}.$$

The last inequality follows from the fact that $l \leq 2d$. This proves the lemma. ■

Lemma 3.3 *If a mesh K (ϵ, η) -approximates S with $\epsilon, \eta < 0.1$ then the following conditions hold:*

- (i) *For any point $k \in K$, $d(k, S) \leq (\epsilon^2 + \epsilon\eta)\rho$.*
- (ii) *For any point $x \in S$, $d(x, K) \leq (\epsilon^2 + \epsilon\eta)\rho$.*
- (iii) *$\phi : K \rightarrow S$ is a homeomorphism.*

Proof: To show (i), consider the figure on the right. Suppose the point k is contained in the triangle $t \in K$ and p is any vertex of t . Let T_p denote the tangent plane at p . Assume that B and B' are the two balls of radius ρ tangentially touching S at p on each side of T_p , and the centers of B and B' are o and o' , respectively.



Recall that n_t is the normal of the triangle t and n_p is the unit surface normal of S at p . Since $\angle(n_p, n_t) < \eta$, the angle between T_p and the plane passing through t is smaller than η , implying that the angle between T_p and the line passing through pk is at most η . Let x denote the projection of k on T_p . We have $\|x - p\| \leq \|k - p\| \leq \epsilon\rho$ and $\|k - x\| \leq \|p - k\| \sin \eta \leq \epsilon\eta\rho$.

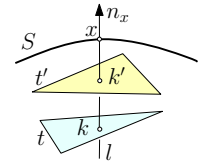
Furthermore, observe that one of the segments xo and xo' must intersect S . Assume without loss of generality that it is xo . Since B does not contain any point from S , we have that $d(x, S) \leq \|x - y\|$ where y is the intersection between xo and B . This implies that

$$d(x, S) \leq \sqrt{\rho^2 + \|x - p\|^2} - \rho \leq \epsilon^2\rho.$$

Since $d(k, S) \leq \|k - x\| + d(x, S)$ by the triangle inequality, Part (i) then follows.

We now show claim (iii), and claim (ii) follows easily from (i) and (iii). Note that by (i), K does not intersect the medial axis of S . Hence the map ϕ is well-defined and actually continuous. Since K is compact, to show (iii), it suffices to show that ϕ is bijective.

First, assume that ϕ is not injective, and it maps two points $k, k' \in K$ to the same point, say $x \in S$. In this case, both k and k' are on the line l passing through x in direction n_x . Without loss of generality, assume that k and k' are two consecutive intersection points between l and K . Let t and t' be the triangles that contain k and k' , respectively. See the right figure for an example. By (i), we have that both $\|k - x\|$ and $\|k' - x\|$ are upper-bounded by $(\epsilon^2 + \epsilon\eta)\rho$.



Consider any vertex p of t . We have that $\|x - p\| \leq \|x - k\| + \|k - p\| \leq (\epsilon + \epsilon^2 + \epsilon\eta)\rho$, by triangle inequality. Since both x and p are in S , we have that $\angle(n_x, n_p) \leq 2\epsilon$ by Lemma 3.1. It then follows that

$$\angle(n_x, n_t) \text{ and } \angle(n_x, n_{t'}) \leq 2\epsilon + \eta. \quad (6)$$

The above equation implies that $t \neq t'$, as otherwise, l lies in the plane passing through t and as such $\angle(n_x, n_t) = \pi/2$, which is not possible. Since k and k' are two consecutive intersection points between L and K , n_x must point to the inside of K at one of these two points, say k . If k lies in the interior of t , then $\angle(n_x, n_t) \geq \pi/2$. Otherwise, k is on the boundary of t , in which case $\angle(n_x, n_t) \geq \pi/2 - 2\eta$ because it follows from the definition of (ϵ, η) -approximation that the neighboring triangle of t forms an angle of at most 2η with t . Either case contradicts Eqn (6). Hence we cannot have two such points k and k' and the map ϕ must be injective.

Finally, note that the image of K under the map ϕ , $\phi(K) \subseteq S$, is a compact surface as well. Since S is connected, by Theorem (7.6) [17], $\phi(K) = S$. It then follows that $\phi : K \rightarrow S$ is a homeomorphism. ■

3.2 Approximating Integrals on the Surface S

Lemma 3.3 implies that the mesh K is close to the underlying surface S both geometrically and topologically. Intuitively, quantities defined on S are closely related to their analogs defined on K (i.e, the pre-images under ϕ). Indeed, consider an arbitrary but fixed triangle $t \in K$. Note that although the map ϕ is not differentiable on the entire domain K , its restriction to the interior of t is differentiable. The following result states that $J(x)$, the *Jacobian* of the map ϕ at an interior point $x \in t$, is close to 1. We note that by elegant differential geometric arguments, Morvan and Thibert [15] and Hildebrandt *et. al.* [12] analyze the Jacobian of ϕ when the meshed surface K is close to S under the Hausdorff distance and normal variation. A bound similar to that in Lemma 3.4 can be derived by combining Lemma 3.3 with their results. For completeness of the exposition we provide a more elementary geometric proof in Appendix B.

Lemma 3.4 *Let K be a triangular mesh that (ϵ, η) -approximates S with $\epsilon, \eta < 0.1$. For any point x in the interior of an arbitrary triangle $t \in K$, we have that $|J(x) - 1| \leq 2(2\epsilon + \eta)^2$. In particular, this implies that the areas of S and K satisfies: $\left| \frac{\text{Area}(S)}{\text{Area}(K)} - 1 \right| \leq 2(2\epsilon + \eta)^2$.*

Proof of Theorem 2.4. Let $g : S \rightarrow \mathbb{R}$ be a function defined on S . We wish to approximate the integral $\int_S g(x) d\nu(x)$ using the values $g(v)$ at vertices v of the mesh K . Specifically, we construct a discrete version of the integral $\int_S g d\nu$ by setting $I_K g = \sum_{t \in K} \frac{\text{Area}(t)}{\#t} \sum_{v \in V(t)} g(v)$, where $\#t$ is the number of vertices in the face t (3 for a triangulation). Intuitively, each face of the mesh contributes the amount equal to its area multiplied by the average value of its vertices.

We prove Theorem 2.4 via the map ϕ . Since ϕ is a homeomorphism, the set of surface mesh faces $\{\phi(t), t \in K\}$ partitions the surface S . Therefore from the change of variable formula we have

$$\int_S g(x) d\nu(x) = \sum_{t \in K} \int_{\phi(t)} g(x) d\nu(x) = \sum_{t \in K} \int_t g(\phi(u, v)) J(u, v) du dv ,$$

where (u, v) is any orthogonal coordinate system on the plane passing through the face t . By Lemma 3.4

$$\begin{aligned} \left| \int_S g(x) d\nu(x) - \sum_{t \in K} \int_t g(\phi(u, v)) dudv \right| &\leq \left| \sum_{t \in K} \int_t g(\phi(u, v)) 2(2\epsilon + \eta)^2 dudv \right| \\ &\leq 2(2\epsilon + \eta)^2 \text{Area}(K) \|g\|_\infty \end{aligned} \quad (7)$$

For any vertex p of t and any point $x = (u, v) \in t$, we have that $\|p - x\| \leq \epsilon\rho$ by definition of (ϵ, η) -approximation. It then follows from Lemma 3.3 (i) and the triangle inequality that $\|p - \phi(x)\| \leq (\epsilon + \epsilon^2 + \epsilon\eta)\rho$. Since $\epsilon, \eta < 0.1$, we have that $d_S(p, \phi(x)) \leq 2\epsilon\rho$ by Lemma 3.2. Hence $|g(\phi(x)) - g(p)| \leq 2\rho L\epsilon$,

where $L = \text{Lip}(g)$ is the Lipschitz constant of g , implying that $|\int_t g(\phi(u, v)) - g(p) dudv| \leq 2\rho L\epsilon \text{Area}(t)$. Combining with Eq. 7 and noticing that p is an arbitrary vertex of t , we have that

$$\left| \int_S g d\nu - \mathbb{I}_K g \right| \leq 2\rho L\epsilon \text{Area}(K) + 2(2\epsilon + \eta)^2 \text{Area}(K) \|g\|_\infty, \quad (8)$$

From Lemma 3.4, we have that $\text{Area}(K) \leq 1.5\text{Area}(S)$. This proves the first part of Theorem 2.4.

In the case when we have a triangular mesh and the function g is twice differentiable, this analysis can be improved to show higher-order convergence. Below we only provide a sketch of the proof due to lack of space. First, consider a twice-differentiable function $h : t \rightarrow \mathbb{R}$ on a triangle $t \in K$, and let p, q, r be the vertices of t . As above, let $x = (u, v)$ be an orthonormal coordinate system on the plane of t . Consider the unique linear function $l(x)$ defined on the plane of the triangle, s.t. $l(p) = h(p), l(q) = h(q), l(r) = h(r)$. It can be shown that $\int_t l(u, v) dudv = \frac{1}{3}(h(p) + h(q) + h(r))\text{Area}(t)$. Without loss of generality assume that p is the origin O of the coordinate system and that $h(p) = 0$ (additive constants will not change the computation). Let $q = (u_1, v_1), r = (u_2, v_2)$. It then follows that

$$l(u, v) = (u \ v) \begin{pmatrix} u_1 & v_1 \\ u_2 & v_2 \end{pmatrix}^{-1} \begin{pmatrix} h(q) \\ h(r) \end{pmatrix}. \quad (9)$$

Writing the Taylor expansion for h with a quadratic remainder term, and recalling that $h(0) = 0$, we have $|h(u, v) - h_u(0)u - h_v(0)v| < H(u^2 + v^2)$, where H is maximum of the norm of the Hessian of h on the triangle, and h_u (resp. h_v) is the partial derivative of h along u (resp. v). Now based on the observation that the function value of a linear function inside a triangle is bounded by the sum of its (absolute) values on the vertices, and that the length of each side of t is at most $\epsilon\rho$, it can be shown that

$$|l(u, v) - h_u(0)u - h_v(0)v| \leq 4H(\epsilon\rho)^2.$$

Combining this with Eqn (9) leads to that $|h(u, v) - l(u, v)| < 5H(\epsilon\rho)^2$. Now set $h(x) = g(\phi(x, y))$. Note that ϕ is infinitely differentiable outside of the medial axis. Then by a standard compactness argument, the second derivative of ϕ , and thus of $g(\phi(x, y))$ (from the chain rule), is bounded. Hence $|g(u, v) - l(u, v)| < CH\epsilon^2$, where C is some constant depending on the geometry of S . Integrating, and using Eqn (7) we obtain

$$\left| \int_S g d\nu - \mathbb{I}_K g \right| \leq CH\epsilon^2 \text{Area}(K) + 2(2\epsilon + \eta)^2 \text{Area}(K) \|g\|_\infty$$

Since $\text{Area}(K) \leq 1.5\text{Area}(S)$, the second part of Theorem 2.4 then follows.

4 Discrete Laplace Operator

We now show our main result (Theorem 2.1) which states that the mesh Laplacian approximates the surface Laplacian well. We first prove Theorem 2.2; that is, given a mesh K (ϵ, η) -approximating a surface S , for any point $w \in S$, the difference between the mesh and the functional Laplace operators $|\mathbb{F}_S^h f(w) - \mathbb{L}_K^h(w)|$ is bounded, and converges to zero as ϵ and η go to 0. Theorem 2.1 then follows from this theorem and Theorem 2.3.

Proof of Theorem 2.2. First, set $g(x) = \frac{1}{4\pi h^2} e^{-\frac{\|x-w\|^2}{4h}} (f(x) - f(w))$. Comparing Eqn (2) and Eqn (1), we obtain that

$$\left| \mathbb{L}_K^h f(w) - \mathbb{F}_S^h f(w) \right| = \left| \int_S g d\nu - \mathbb{I}_K g \right| \quad (10)$$

By (the first part of) Theorem 2.4, to bound the above quantity, it suffices to bound $\|g\|_\infty$ and the Lipschitz constant $\text{Lip}(g)$ of g . Easy to verify that $\|g\|_\infty \leq \frac{1}{2\pi h^2} \|f\|_\infty$. For $\text{Lip}(g)$, since f , and thus g , is C^1 -continuous, it is upper bounded by $\|g'\|_\infty = \sup_{x \in S} \|g'(x)\|$. Notice that $g'(x)$ is a map from the tangent space T_x to \mathbb{R} . By definition, $g'(x)(v) = \nabla_S g(x) \cdot v$ for any vector $v \in T_x$ and hence $\|g'(x)\| = \|\nabla_S g(x)\|$. On the other hand, it is easy to verify that

$$\|\nabla_S g(x)\| \leq \frac{1}{4\pi h^2} (2\|f\|_\infty \cdot \|\nabla_S e^{-\frac{\|x-w\|^2}{4h}}\| + \|\nabla_S f(x)\|).$$

Since S is a surface embedded in \mathbb{R}^3 with the induced Riemannian metric, it holds that

$$\|\nabla_S e^{-\frac{\|x-w\|^2}{4h}}\| \leq \|\nabla_{\mathbb{R}^3} e^{-\frac{\|x-w\|^2}{4h}}\| = e^{-\frac{\|x-w\|^2}{4h}} \|x-w\|/(2h) \leq \frac{1}{\sqrt{h}}$$

where the last inequality holds as $y/e^{y^2} \leq 1$ for any real number y . It then follows that

$$\|g'\|_\infty = \|\nabla_S g(x)\| \leq \frac{1}{4\pi h^2} \left(\frac{2\|f\|_\infty}{\sqrt{h}} + \|f'\|_\infty \right).$$

Combining with Theorem 2.4, and putting everything together, we conclude with Theorem 2.2.

Proof of Theorem 2.1. Now let $K_{\varepsilon,\eta}$ denote an (ε, η) -approximation of S with $\varepsilon, \eta < 0.1$, and $h(\varepsilon, \eta)$ an appropriate constant depending on ε and η . We have that for any point $w \in S$,

$$\left| \mathbb{L}_{K_{\varepsilon,\eta}}^{h(\varepsilon,\eta)} f(w) - \Delta_S f(w) \right| \leq \left| \mathbb{L}_{K_{\varepsilon,\eta}}^{h(\varepsilon,\eta)} f(w) - \mathbb{F}_S^{h(\varepsilon,\eta)} f(w) \right| + \left| \mathbb{F}_S^{h(\varepsilon,\eta)} f(w) - \Delta_S f(w) \right|.$$

By choosing $h(\varepsilon, \eta) = \frac{1}{\varepsilon^{2.5+\alpha}} + \frac{1}{\eta^{1+\alpha}}$, where $\alpha > 0$ is an arbitrary fixed positive number, it can be shown

$$\left| \mathbb{L}_{K_{\varepsilon,\eta}}^{h(\varepsilon,\eta)} f(w) - \Delta_S f(w) \right| \leq O(\varepsilon^{\frac{\alpha}{2.5+\alpha}}) + O(\eta^{\frac{\alpha}{1+\alpha}}) + |\mathbb{F}_S^{h(\varepsilon,\eta)} f(w) - \Delta_S f(w)|$$

The big-O notation above hides terms linear in the area $\text{Area}(S)$, the reach $\rho(S)$, $\|f\|_\infty$ and $\|f'\|_\infty$. The limit $\lim_{t \rightarrow 0} |\mathbb{F}_S^{h(\varepsilon,\eta)} f(w) - \Delta_S f(w)| = 0$ by Theorem 2.3 ([7]).

By taking the limit, we see that $\lim_{\varepsilon, \eta \rightarrow 0} \mathbb{L}_{K_{\varepsilon,\eta}}^{h(\varepsilon,\eta)} f(w) = \Delta_S f(w)$, which proves Theorem 2.1.

5 Experiments

In this section, we apply our algorithm of computing the mesh Laplacian to different surfaces and show its convergence as the mesh becomes finer. One currently widely used mesh Laplace operator is the *cotangent* (COT) *scheme*, originally proposed by Pinkall and Polthier [18]. We compare our algorithm with its modified version [14, 24], which produces better results than the original method. Our experiments show that the COT scheme does not produce convergence for functions other than linear functions, while our method, in addition to exhibiting convergence behavior, is also much more robust with respect to noisy data.

Experimental setup. To analyze the convergence behavior, we need the “ground truth”, that is, we need to know the Laplace-Beltrami operator for the underlying surface approximated by input meshes. This somewhat limits the type of surfaces that we can experiment with. In this paper, we consider two types of surfaces: planar surfaces and spherical surfaces. For the planar surface, we uniformly sample the region $[-1, 1] \times [-1, 1]$ with different density, and construct the Delaunay triangulation for the resulting sample points. For the spherical surface, we sample a unit sphere, either uniformly or non-uniformly, with different density, and then use the COCONE software [4] to generate the triangular meshes. The goal of the non-uniform sampling is to create “bad” meshes, such as those with skinny triangles and triangles of different sizes. We also produce noisy data from the uniform sampling of the sphere, by perturbing each sample point randomly by a small shift. Some examples of these three types of spherical meshes are shown in Figure 1.

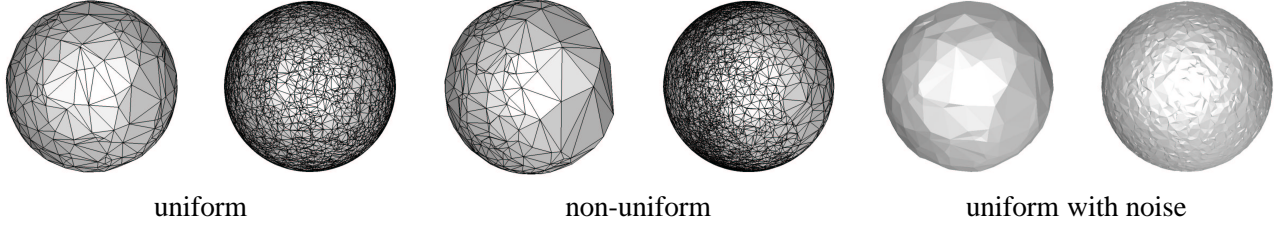


Figure 1: Meshes for spherical surface with 500 sample points and 8000 sample points.

Error measure. Given a mesh K approximating a surface S and an input function $f : S \rightarrow \mathbb{R}$, we evaluate the surface Laplacian and the mesh Laplacian at each of the n vertices of K , and obtain two n dimensional vectors U and \widehat{U} , respectively. To measure the error between the mesh Laplacian and the surface Laplacian, we consider the commonly used normalized L_2 error $E_2 = \frac{\|U - \widehat{U}\|_2}{\|U\|_2}$. We remark that our theoretical result is that our mesh Laplacian converges under the L_∞ norm (i.e. point-wise convergence), which is a stronger result than the L_2 -convergence (as L_∞ -convergence implies L_2 -convergence). Such convergence is indeed observed for all types of meshes that we have conducted experiments on. However, since the COT scheme performs poorly under the L_∞ error metric, we only show results under the L_2 error metric from now on — our method compares even more favorably under the L_∞ error.

Results for planar surface. Given a function $f : \mathbb{R}^2 \rightarrow \mathbb{R}$ on the plane, its surface Laplacian is simply: $\Delta_{\mathbb{R}^2} f(x, y) = \frac{\partial^2 f}{\partial x^2} + \frac{\partial^2 f}{\partial y^2}$. Specifically, $\Delta_{\mathbb{R}^2} f(x, y) = 0$ if f is a linear function. It turns out that the COT scheme produces exactly 0 for a linear function on a planar mesh. Hence we compare the mesh Laplacians for two non-linear functions: $f(x, y) = x^2$ and $f(x, y) = e^{x+y}$. The results under the normalized L_2 error metric are shown in Table 1. For both functions, for different values of the parameter h , our method always presents convergence behavior; while finer mesh does not lead to lower approximation error by the COT scheme. Note that we obtain better approximation even when the number of sample points is small (500). Since different values of h show similar behavior, from now on, we fix the parameter at $4h = 0.04$.

Method	Param	500	2000	8000	16000	500	2000	8000	16000
COT	non	0.220	0.173	0.197	0.207	0.198	0.188	0.190	0.202
OUR	4h=0.01	0.450	0.146	0.040	0.022	0.875	0.128	0.055	0.027
	4h=0.04	0.126	0.038	0.010	0.005	0.189	0.037	0.022	0.016
	4h=0.09	0.069	0.017	0.004	0.002	0.099	0.033	0.027	0.025
$f = x^2$						$f = \exp(x + y)$			

Table 1: Normalized L_2 error for planar mesh. We show the results of our method with there different h values.

Spherical surfaces. Given a function $f : \mathbb{S}^2 \rightarrow \mathbb{R}$ defined on the unit sphere \mathbb{S}^2 , where f is parametrized by the spherical coordinates θ and ϕ , its spherical surface Laplacian is:

$$\Delta_{\mathbb{S}^2} f(\theta, \phi) = \frac{1}{\sin \theta} \frac{\partial}{\partial \theta} \left(\sin \theta \frac{\partial f}{\partial \theta} \right) + \frac{1}{\sin^2 \theta} \frac{\partial^2 f}{\partial \phi^2}.$$

Xu [24] proved that his modification of the COT scheme can produce convergent result for linear function defined on spheres. Indeed, this is observed in our experimental results as shown in Table 2, where we also compare the mesh Laplacians for two non-linear functions $f(x, y, z) = x^2$ and $f(x, y, z) = e^x$ for a uniformly sampled spherical mesh. However, while our method converges for all the three functions, the COT scheme only converges under the linear function. In Table 2, we also show the approximation error of

Method	500	2000	8000	16000	500	2000	8000	16000	500	2000	8000	16000
COT	0.058	0.030	0.015	0.011	0.171	0.157	0.158	0.155	0.124	0.101	0.102	0.099
OUR	0.606	0.142	0.034	0.017	0.488	0.115	0.013	0.005	0.613	0.140	0.028	0.015
L_2	$f = x$				$f = x^2$				$f = \exp(x)$			
Method	500	2000	8000	16000	500	2000	8000	16000	500	2000	8000	16000
COT	0.229	0.185	0.083	0.062	1.147	1.577	1.478	1.375	0.798	0.887	0.928	0.849
OUR	2.097	0.492	0.081	0.037	2.915	0.838	0.062	0.025	4.000	0.873	0.112	0.054
L_∞	$f = x$				$f = x^2$				$f = \exp(x)$			

Table 2: Normalized L_2 error (top table) and L_∞ error (bottom table) for spherical meshes with uniform sampling.

the two mesh Laplacians under the L_∞ error metric. Note that compared to the case of normalized L_2 error, the numerical values of L_∞ error can be big, as it is the absolute error and not normalized.

We also test the COT scheme and our mesh Laplacian for meshes constructed from points non-uniformly sampled from the unit sphere. The error obtained for both methods are fairly similar to that on the regular mesh (as reported in Table 2). We omit the detailed results due to lack of space.

Finally, in Table 3, we show how our method and the COT scheme perform for noisy data. Note that even though the COT scheme has been proven to converge for linear functions on a sphere, once the mesh becomes noisy, such convergence behavior is lost; while the approximation error by our algorithm stays almost the same as before. This is not too surprising as our scheme considers a much larger neighborhood than COT scheme when evaluating the mesh Laplacian at a point, which has the “smoothing” effect. However, it is not clear how to extend COT scheme to incorporate larger neighborhood than its current one-ring neighborhood.

Method	500	2000	8000	16000	500	2000	8000	16000	500	2000	8000	16000
COT	0.398	1.532	3.015	0.936	0.267	0.914	1.840	0.545	0.308	1.271	2.631	0.817
OUR	0.599	0.155	0.051	0.022	0.484	0.128	0.028	0.006	0.612	0.153	0.043	0.018
	$f = x$				$f = x^2$				$f = \exp(x)$			

Table 3: Normalized L_2 error for the experiments on the sphere with noise.

Remark. Finally, we remark that we have also compared our mesh Laplacian with the graph Laplacian. Graph Laplacian has been shown to converge for *points randomly sampled from the uniform distribution on the underlying manifold* [7], which is also observed in our experiments when points are randomly sampled. However, our mesh Laplacian produces consistently smaller errors. For non-uniformly sampled meshes, graph Laplacian is not expected to converge to the surface Laplacian.

6 Conclusions

In this paper, we have developed the first algorithm for approximating the Laplace operator on a meshed surface with point-wise convergence guarantee. Such convergence is required in many applications, where quantities, such as mean curvature, need to be estimated at each node of the mesh. The convergence result does not require the aspect ratio of mesh elements to be bounded. Experimental results show that our algorithm indeed exhibits convergence empirically, and outperforms current popular methods both in accuracy and in its robustness with respect to noisy data. To provide theoretical analysis of our algorithm, we also established a general result to compare integrals over a smooth surface and their discretization on a mesh.

Future directions include extending current algorithm to adapt the local mesh size, establishing convergence results for high dimension meshes, as well as developing the theoretical framework for analyzing noisy data.

References

- [1] Discrete differential geometry: An applied introduction. SIGGRAPH 2005 / 2006 course notes.
- [2] P. Alliez, M. Meyer, and M. Desbrun. Interactive geometry remeshing. In *SIGGRAPH '02: Proceedings of the 29th annual conference on Computer graphics and interactive techniques*, pages 347–354, New York, NY, USA, 2002. ACM Press.
- [3] N. Amenta and M. Bern. Surface reconstruction by voronoi filtering. *Discr. Comput. Geom.*, 22:481–504, 1999.
- [4] N. Amenta, S. Choi, T. K. Dey, and N. Leekha. A simple algorithm for homeomorphic surface reconstruction. *Internat. J. Comput. Geom. & Applications*, 12:125–141, 2002.
- [5] N. Amenta and T. K. Dey. Normal variation with adaptive feature size. <http://www.cse.ohio-state.edu/~tamaldey/papers.html>, 2007.
- [6] M. Belkin and P. Niyogi. Laplacian eigenmaps for dimensionality reduction and data representation. *Neural Computation*, 15(6):1373–1396, 2003.
- [7] M. Belkin and P. Niyogi. Towards a theoretical foundation for laplacian-based manifold methods. In *COLT*, pages 486–500, 2005.
- [8] L. Demanet. Painless, highly accurate discretizations of the laplacian on a smooth manifold. Technical report, Stanford University, 2006.
- [9] M. Desbrun, M. Meyer, P. Schröder, and A. H. Barr. Implicit fairing of irregular meshes using diffusion and curvature flow. *Computer Graphics*, 33(Annual Conference Series):317–324, 1999.
- [10] T. K. Dey. *Curve and Surface Reconstruction: Algorithms with Mathematical Analysis (Cambridge Monographs on Applied and Computational Mathematics)*. Cambridge University Press, New York, NY, USA, 2006.
- [11] S. Dong, P.-T. Bremer, M. Garland, V. Pascucci, and J. C. Hart. Spectral surface quadrangulation. In *SIGGRAPH '06: ACM SIGGRAPH 2006 Papers*, pages 1057–1066, New York, NY, USA, 2006. ACM Press.
- [12] K. Hildebrandt, K. Polthier, and M. Wardetzky. On the convergence of metric and geometric properties of polyhedral surfaces. *Geometriae Dedicata*, 123(1):89–112, December 2006.
- [13] U. F. Mayer. Numerical solutions for the surface diffusion flow in three space dimensions. *comput. Appl. Math*, 20(3):361–379, 2001.
- [14] M. Meyer, M. Desbrun, P. Schröder, and A. H. Barr. Discrete differential geometry operators for triangulated 2-manifolds. In *Proc. VisMath'02*, Berlin, Germany, 2002.
- [15] J.-M. Morvan and B. Thibert. Approximation of the normal vector field and the area of a smooth surface. *Discrete & Computational Geometry*, 32(3):383–400, 2004.
- [16] P. Niyogi, S. Smale, and S. Weinberger. Finding the homology of submanifolds with high confidence from random samples. *Discrete and Computational Geometry*, 2006.
- [17] B. O’Neil. *Elementary Differential Geometry*. Academic Press, New York, NY, USA, 1966.

- [18] U. Pinkall and K. Polthier. Computing discrete minimal surfaces and their conjugates. *Experimental Mathematics*, 2(1):15–36, 1993.
- [19] S. Rosenberg. *The Laplacian on a Riemannian Manifold: An Introduction to Analysis on Manifolds*. Cambridge University Press, 1997.
- [20] O. Sorkine. Differential representations for mesh processing. *Computer Graphics Forum*, 25(4):789–807, 2006.
- [21] O. Sorkine, Y. Lipman, D. Cohen-Or, M. Alexa, C. Rössl, and H.-P. Seidel. Laplacian surface editing. In *Proceedings of the Eurographics/ACM SIGGRAPH Symposium on Geometry Processing*, pages 179–188. ACM Press, 2004.
- [22] G. Taubin. A signal processing approach to fair surface design. In *SIGGRAPH '95: Proceedings of the 22nd annual conference on Computer graphics and interactive techniques*, pages 351–358, New York, NY, USA, 1995. ACM Press.
- [23] M. Wardetzky. Convergence of the cotangent formula: An overview. In A. I. Bobenko, J. M. Sullivan, P. Schröder, and G. Ziegler, editors, *Discrete Differential Geometry*, pages 89–112. Birkhäuser, to appear.
- [24] G. Xu. Discrete laplace-beltrami operators and their convergence. *Comput. Aided Geom. Des.*, 21(8):767–784, 2004.
- [25] G. Xu. Convergence analysis of a discretization scheme for gaussian curvature over triangular surfaces. *Comput. Aided Geom. Des.*, 23(2):193–207, 2006.
- [26] K. Zhou, J. Huang, J. Snyder, X. Liu, H. Bao, B. Guo, and H.-Y. Shum. Large mesh deformation using the volumetric graph laplacian. *ACM Trans. Graph.*, 24(3):496–503, 2005.

A Functional approximation of the Laplace-Beltrami operator

In this appendix we attempt to demystify Theorem 2.3 by explaining the underlying idea for the functional approximation of the Laplacian. The core of the approximation theorem lies in the connection of the Laplace-Beltrami operator to the heat equation.

Recall, that given a twice differentiable function $f \in C^2(S)$, let $\nabla_S f$ be the gradient vector field of f on S . The Laplace-Beltrami operator Δ_S applied to f can be defined as the divergence of the gradient; that is, $\Delta_S f = \text{div}(\nabla_S f)$. If S is a domain in \mathbb{R}^2 , the Laplacian has the familiar form $\Delta_{\mathbb{R}^2} f = \frac{\partial^2 f}{\partial x^2} + \frac{\partial^2 f}{\partial y^2}$

The *heat equation* on the surface S is the partial differential equation

$$\Delta_S f(x, t) = \frac{\partial f}{\partial t}(x, t)$$

The heat equation describes the diffusion of the initial heat distribution $f(x, 0)$ at time t . To obtain an integral approximation for the Laplace operator, we use a functional approximation technique from [6]. The approximation is based on the properties of heat propagation with the initial distribution $f(x) = f(x, 0)$. It is well known (e.g., [19]) that the solution to the heat equation $f(x, t)$ can be written as $f(x, t) = \int_S H_S^t(x, y) f(y) d\nu(y)$, where $H_S^t(x, y)$ is the *heat kernel* of the surface S , i.e. the measure of how much heat propagates from x to y in time t . The quantity $\int_S H_S^t(x, y) f(y) d\nu(y)$ can be thought of as the sum of all heat coming to point x from every other point y after time t .

Thus the heat equation can be rewritten as follows:

$$\Delta_S f(x, t) = \int_S H_S^t(x, y) f(y) d\nu(y)$$

Taking the limit as $t \rightarrow 0$ and recalling that $f(x, 0) = f(x)$ and that $\int H_S^t(x, y) d\nu(y) = 1$, yields

$$\begin{aligned} \Delta_S f(x) &= \lim_{t \rightarrow 0} \int_S H_S^t(x, y) f(y) d\nu(y) = \\ \lim_{t \rightarrow 0} \frac{1}{t} \left(\int_S H_S^t(x, y) f(y) d\nu(y) - f(x) \right) &= \\ \lim_{t \rightarrow 0} \frac{1}{t} \int_S H_S^t(x, y) (f(y) - f(x)) d\nu(y) & \end{aligned}$$

For the case when S is \mathbb{R}^N the heat kernel can be written explicitly $H_{\mathbb{R}^2}^t(x, y) = \frac{1}{\sqrt{(4\pi t)}} \exp\left(-\frac{\|x-y\|^2}{4t}\right)$, yielding the functional approximation in Eq. 2.

For a general manifold, the heat kernel cannot usually be written explicitly. However the heat kernel can be shown to be close to a Gaussian in the geodesic coordinates (e.g., [19]). By considering the asymptotes of the heat kernel as $t \rightarrow 0$, the result in Theorem 2.3 can still be established (see [7]).

B Jacobian of ϕ

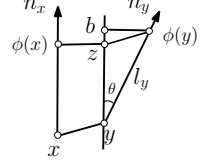
For any point $x \in t$, let \hat{n}_x be the surface normal at $\phi(x)$; that is, $\hat{n}_x = n_{\phi(x)}$. The following lemma from [5] says that the rate that \hat{n}_x changes as x moves around in t is bounded.

Lemma B.1 *Let K be a triangular mesh that (ϵ, η) -approximates S with $\epsilon, \eta < 0.1$. Given any triangle $t \in K$, for any x in the interior of t , and for any unit vector v in the plane passing through t , we have that*

$$\left| \lim_{\delta \rightarrow 0} \frac{\angle(\hat{n}_{x+\delta v}, \hat{n}_x)}{\delta} \right| \leq \frac{1}{(1-\epsilon)\rho},$$

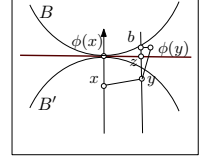
Proof of Lemma 3.4. Let P be the plane where the triangle t lies, and $T_{\phi(x)}$ be the tangent plane of S at $\phi(x)$. Set α denote the angle between the planes P and $T_{\phi(x)}$. Note that $\alpha < 2\varepsilon + \eta$ by Eqn (6). Easy to see that there exists an orthogonal coordinate system (u, v) on P such that $\angle(u, T_{\phi(x)}) = \alpha$ and $\angle(v, T_{\phi(x)}) = 0$. Let $\phi_u(x)$ and $\phi_v(x)$ be the partial derivatives of ϕ at a point $x = (u_0, v_0)$ in the interior of t , respectively. The Jacobian $J(x) = J(u_0, v_0)$ of ϕ at x then equals $\sqrt{EG - F^2}$, where $E = \phi_u \cdot \phi_u$, $G = \phi_v \cdot \phi_v$ and $F = \phi_u \cdot \phi_v$.

To bound ϕ_u , consider the point $y = (u_0 + \delta, v_0)$, where δ is a real number. Note that by the choice of the direction u , the angle $\angle((y - x), T_{\phi(x)})$ between $y - x$ and the plane $T_{\phi(x)}$ is α . Let z be the projection point of y onto $T_{\phi(x)}$ and b be the projection of $\phi(y)$ onto the line yz . See the right figure. Set $\theta = \angle(\hat{n}_x, \hat{n}_y)$; note that $\theta \leq \frac{\delta}{(1-\varepsilon)\rho}$ by Lemma B.1. Since $\|\phi(y) - y\| \leq (\varepsilon^2 + \varepsilon\eta)\rho$ by Lemma 3.3, we have that



$$\|\phi(y) - b\| = \|\phi(y) - y\| \cos \theta < \frac{\varepsilon^2 + \varepsilon\eta}{1 - \varepsilon} |\delta|$$

Now let B and B' be the two balls of radius ρ that tangentially touch S at $\phi(x)$. By the definition of the reach ρ , the surface S has to lie outside these two balls. It can be shown that $\|b - z\|$ is of order δ^2 . Hence



$$\lim_{\delta \rightarrow 0} \frac{\|z - \phi(y)\|}{|\delta|} \leq \lim_{\delta \rightarrow 0} \frac{\|z - b\| + \|b - \phi(y)\|}{|\delta|} \leq \frac{\varepsilon^2 + \varepsilon\eta}{1 - \varepsilon} \quad (11)$$

By definition, $\sqrt{E} = \lim_{\delta \rightarrow 0} \frac{\|\phi(x) - \phi(y)\|}{|\delta|}$. Consider the triangle consisting of $\phi(x)$, $\phi(y)$ and z . Since $\|\phi(x) - z\| = \|y - x\| = \delta \cos \alpha$, it follows from the triangle inequality and Eqn (11) that

$$|\sqrt{E} - 1| \leq (1 - \cos \alpha) + \frac{\varepsilon^2 + \varepsilon\eta}{1 - \varepsilon}.$$

Furthermore, let α_u be the angle between the vectors $z - \phi(x)$ and ϕ_u (i.e., $\phi(y) - \phi(x)$). We have for small enough δ that

$$\sin \alpha_u \leq \frac{\|z - \phi(y)\|}{\|z - \phi(x)\|} \leq \frac{\varepsilon^2 + \varepsilon\eta}{(1 - \varepsilon) \cos \alpha}.$$

Similarly, let $w = (u_0, v_0 + \delta)$ and z' the projection of w onto the plane $T_{\phi(x)}$. Let $\alpha_v = \angle((z' - \phi(x)), \phi_v)$. Similar argument can show that

$$|\sqrt{G} - 1| \leq \frac{\varepsilon^2 + \varepsilon\eta}{1 - \varepsilon} \quad \text{and} \quad \sin \alpha_v \leq \frac{\|z - \phi(y)\|}{\|z - \phi(x)\|} \leq \frac{\varepsilon^2 + \varepsilon\eta}{(1 - \varepsilon)}.$$

Finally, observe that by the triangle inequality,

$$|\angle(\phi_u, \phi_v) - \pi/2| \leq (\alpha_u + \alpha_v).$$

Since $|F| = \sqrt{EG} |\cos \angle(\phi_u, \phi_v)|$, it follows that

$$\sqrt{EG} (1 - \cos^2 \angle(\phi_u, \phi_v)) \leq \sqrt{EG - F^2} \leq \sqrt{EG}$$

and the lemma follows from the bounds derived for E, G, α_u, α_v .